RESEARCH/REVIEW ARTICLE

Coastal glaciers advanced onto Jameson Land, East Greenland during the late glacial–early Holocene Milne Land Stade

Helena Alexanderson[1] & Lena Håkansson[2,3]

[1] Department of Geology, Lund University, Sölvegatan 12, SE-223 62 Lund, Sweden
[2] Geological Survey of Denmark and Greenland, Marine Geology and Glaciology, Østervoldgade 10, DK-1350 Copenhagen K, Denmark
[3] Department of Geology and Mineral Resources Engineering, Norwegian University of Science and Technology, Sem Særlands veg 1, NO-7491 Trondheim, Norway

Keywords
Greenland; Jameson Land; glaciation; Milne Land Stade; cosmogenic exposure dating; luminescence dating.

Correspondence
Lena Håkansson, Geological Survey of Denmark and Greenland, Marine Geology and Glaciology, Østervoldgade 10, DK-1350 Copenhagen K, Denmark.
E-mail: lena.hakansson@geol.lu.se

Abstract

We report on ^{10}Be and optically stimulated luminescence ages from moraines and glaciolacustrine sediments on eastern Jameson Land, East Greenland. Sampled landforms and sediment are associated with advances of outlet glaciers from the local Liverpool Land ice cap situated in the coastal Scoresby Sund region. Previous studies have tentatively correlated these advances with the Milne Land Stade moraines, which are prominent moraine sets deposited by mountain glaciers in the inner Scoresby Sund region. Recent constraints on the formation of the outer and inner of these moraines have suggested two advances of local glaciers, one prior to or during the Younger Dryas and another during the Preboreal. In this paper, we test the correlation of the Liverpool Land glacial advance with the Milne Land Stade. Our results show that outlet glaciers from the Liverpool Land ice cap reached ice-marginal positions marked by moraines in east-facing valleys on Jameson Land sometime during late glacial–early Holocene time (ca. 13–11 Kya). This confirms the correlation of these moraines with the Milne Land Stade moraines described elsewhere in the Scoresby Sund region.

Local glaciers are sensitive recorders of climate change (e.g., Nesje et al. 2008; Carr et al. 2010; Leclercq & Oerlemans 2012) in comparison with ice sheets and ice-sheet margins, which may have a longer response time. Geological records from Greenland show that local glaciers and ice caps advanced and retreated partly out of tune with the Greenland Ice Sheet during the last glacial/interglacial cycle (Adrielsson & Alexanderson 2005; Kelly & Lowell 2009). The rapid climate change during the last termination has been of particular interest, and studies of moraines or other landforms demarcating local glacial extent during that time may provide information on climate factors such as precipitation and temperature (see Kelly & Lowell 2009).

In East Greenland, one such feature is the prominent Milne Land Stade moraines, originally described by Funder (1970). The moraines consist of an outer and an inner belt, and they are exposed widely in the central parts of the Scoresby Sund region, on Milne Land and in Hall Bredning (Fig. 1). Even though these moraines are the only prominent ice-marginal features between the last glacial maximum and little ice age ice-marginal positions, their age has been debated. Originally they were assigned a Younger Dryas age (Funder 1972, 1978). However, subsequent studies have suggested deposition during Preboreal time (Funder & Hansen 1996; Björck et al. 1997). The latter alternative was favoured because it has long been thought that the Younger Dryas was too cold and dry to accommodate glacier growth (Funder & Hansen 1996). Recent studies of the inner and outer Milne Land Stade moraines in the inner Scoresby Sund area place the outer Milne Land Stade prior to or during the Younger Dryas and the inner Milne Land Stade in the Preboreal, based on relative sea-level data and exposure ages of moraines (Hall et al. 2008; Kelly et al. 2008).

The Milne Land Stade moraines have been tentatively correlated with fresh-looking moraines on eastern Jameson Land adjacent to former outlets of a Liverpool

Citation: *Polar Research* 2014, *33*, 20313, http://dx.doi.org/10.3402/polar.v33.20313

Polar Research

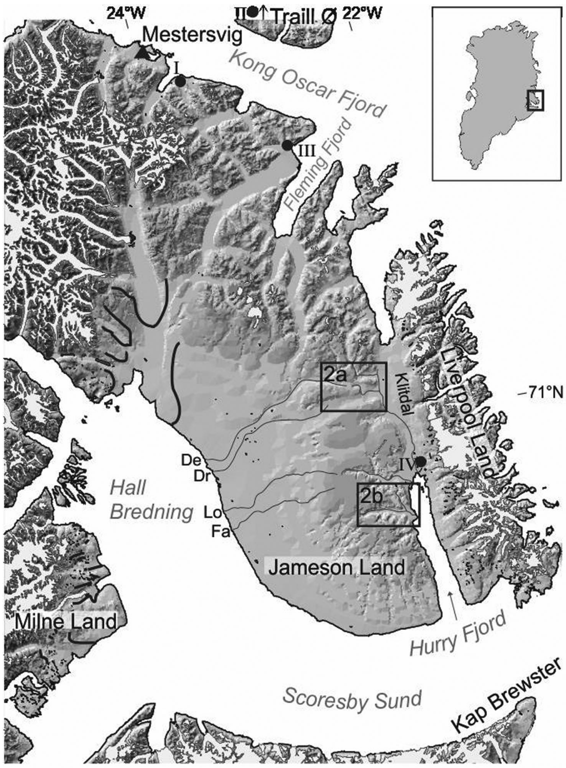

Fig. 1 Map of Greenland and the Scoresby Sund–Jameson Land area. The open squares mark our study areas (see Fig. 2). The filled triangle represents the Mestersvig delta and the filled circles with roman numbers the positions of radiocarbon samples (see Table 2 for site numbers). Thick black lines represent Milne Land Stade moraines as described by Funder (1970) in Milne Land and by Denton et al. (2005) north of Hall Bredning. The following river names are abbreviated: Depotelv (De), Draba Sibirica Elv (Dr), Lollandselv (Lo) and Falsterselv (Fa) rivers. Copyright background map: National Survey and Cadastre, Denmark.

Land-based ice cap (Funder 1990; Lillieskold & Salvigsen 1991). No absolute ages are available for these moraines, but from the stratigraphic record we know that glaciers on Liverpool Land advanced onto eastern Jameson Land at least twice during the last two glacial cycles: two tills are placed in the Saalian (170–150 Kya) and in the Weichselian (100–10 Kya), respectively (Adrielsson & Alexanderson 2005).

In this paper, we attempt to test the correlation of the youngest Liverpool Land advance with the Milne Land Stade, as proposed by Funder (1990), among others. To do so, we apply cosmogenic ^{10}Be dating to constrain the age of moraines and optically stimulated luminescence (OSL) to date glacial lake sediments associated with these ice-marginal positions in four valleys in eastern Jameson Land. We further want to reconstruct depositional environments associated with the westward advance of Liverpool Land glaciers. This is done through sedimentological descriptions and logging of glacially associated landforms in eastern Jameson Land valleys.

Geological setting

The Jameson Land peninsula (70°–71°N) is located at the northern side of Scoresby Sund, the largest fjord system in East Greenland (Fig. 1). The distance between the fjord mouth and the present margin of the Greenland Ice Sheet is about 200 km. Mesozoic sandstones and shales make up the low-relief ice-free terrain in Jameson Land. The peninsula has an asymmetric topographic profile; from the Scoresby Sund coast the terrain rises gently towards the plateau areas of interior Jameson Land, ca. 500 m a.s.l., whereas in the east the plateau margins drop steeply (Fig. 1). The central plateau is dissected by fluvial erosion that has created a radiating drainage pattern from central Jameson Land towards the Scoresby Sund and Hurry Fjord coasts. Liverpool Land is situated at the outer coast and is separated from Jameson Land to the west by the Hurry Fjord and the Klitdal valley. The crystalline terrain of Liverpool Land is characterized by an alpine topography with local glaciers and small ice caps.

Earlier studies have suggested that the interior of Jameson Land was ice-free during the last glacial cycle and that the last advance of the Greenland Ice Sheet overriding the peninsula occurred during Marine Isotope Stage (MIS) 6 (Funder et al. 1994, 1998; Möller et al. 1994). This was based on the weathered appearance of the central plateau areas of the peninsula and the lack of glacial deposits of Weichselian age. However, studies applying cosmogenic exposure dating to erratics perched at 250 m a.s.l. on the Kap Brewster Peninsula at the mouth of the Scoresby Sund fjord indicate that ice reached more than 250 m above the present sea level during the last glacial maximum. This suggests that the Greenland Ice Sheet was considerably more extensive during this time than previously thought (Håkansson et al. 2007).

In most of the east-facing valleys on eastern Jameson Land, there are prominent moraine ridges which are concave towards the east and reflect former ice-marginal positions of outlet glaciers from the Liverpool Land ice cap. These moraines have been tentatively assigned to the Milne Land Stade (Funder 1972). Further, they were mapped from aerial photographs and shown on the Quaternary map of Scoresby Sund (Funder 1990). Series of deltas deposited in lakes dammed during these glacier advances have also been described from some of these valleys (Lillieskold & Salvigsen 1991).

In this study, we have investigated four valleys in two different areas on eastern Jameson Land. In the Lejrelv

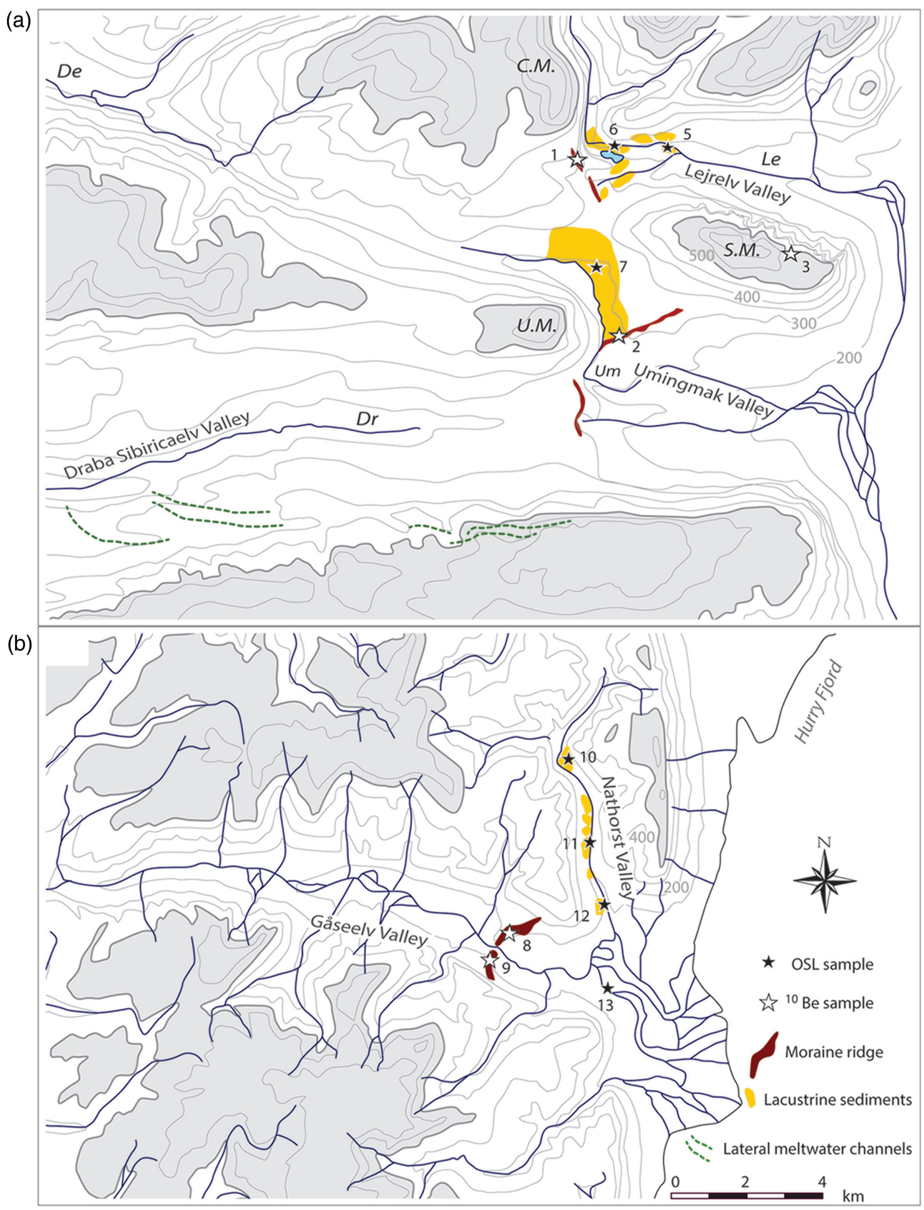

Fig. 2 Maps showing the study areas: (a) the Lejrelv area (contour interval of 50 m); (b) the Gåseelv area (contour interval of 100 m). The bold line marks the 500 m contour and light grey areas show terrain above 500 m a.s.l. Stars mark the sites from which samples for ^{10}Be (white) and optically stimulated luminescence (OSL; black) dating have been taken and numbers refer to site numbers (Table 1). The geomorphological features are based on the maps by Lilliesköld & Salvigsen (1991) and our field survey. Topographic information is from copyright, National Survey and Cadastre, Denmark. The following river names are abbreviated: Depotelv (De), Draba Sibirica Elv (Dr), Lejrelv (Le) and Umingmelv (Um). The following names of mountains are abbreviated: Centralbjerg (C.M.); Skansen (S.M.) and Umingmak (U.M.).

area (Fig. 2a), the Lejrelv and Umingmakelv valleys (informal names) are situated about 5 km apart, approximately 30 km north of the head of Hurry Fjord (Fig. 1). These east-facing valleys run parallel to each other. They are bounded to the north and south by flat-topped mountains made up by weathered Mesozoic sandstone that reach above 500 m a.s.l.: the Centralbjerg mountain to the north, the Skansen and Umingmak mountains between the valleys and a nameless mountain to the south (Fig. 2a). The Lejrelv and Umingmakelv rivers make sharp turns towards the east and drain through deep canyons as they enter their valleys (Fig. 2a). The modern-day rivers are underfit to the >50 m deep canyons, which were most likely incised by glacial meltwater. The water divide is situated within 15 km of the valley mouths (Fig. 2a). The Lejrelv Valley is relatively narrow and constrained by the eastern flank of the Centralbjerg mountain. In contrast, the Umingmakelv Valley to the south is wider and directly connected to the Draba Sibiricaelv Valley on the western side of the water divide (Figs. 1, 2a).

In the Gåseelv area, the Gåseelv Valley and its tributary the Nathorst Valley (informal name) are situated ca. 3 km south of the head of the Hurry Fjord (Fig. 2b). The Gåseelv Valley is an east-facing valley bounded by mountains reaching ca. 450–700 m a.s.l. The Nathorst Valley stretches north–south and connects with the Gåseelv Valley ca. 1.5 km to the west of the Hurry Fjord coast (Fig. 1). The east–west water divide in the Gåseelv Valley is situated less than 20 km from the Hurry Fjord coast.

Samples and methods

Fieldwork

Fieldwork was carried out during the summer 2005 and included geomorphological surveys in the study areas, sedimentological logging at selected sites and sampling for cosmogenic exposure dating and OSL dating. The investigated sites included seven in the Lejrelv area and six in the Gåseelv area (Table 1). Positions and elevations were determined by a handheld global positioning system (GPS) device (uncertainty ± 10 m). Our elevations appear to differ from those described for the same landforms by Lilliesköld & Salvigsen (1991), but the difference is within the uncertainty of the GPS device. In this study, we consistently use our elevations.

Cosmogenic exposure dating

A total of eight samples were collected, six of which are amalgamated pebble samples. Each pebble sample contains 20 clasts of approximately the same size. Sample thickness is equal to the average diameter of pebbles. Samples were collected from flat, well-drained surfaces about 4×4 m in area. Shielding from the surrounding horizon was measured with a compass and clinometer. Samples were processed for ^{10}Be analysis at the University at Buffalo following procedures modified from Kohl & Nishiizumi (1992) and Briner (2003). About 40 g of clean quartz from each sample was dissolved in batches of 11 and one process blank (Table 3). Known amounts of SPEX CertiPrep (Metuchen, NJ, USA) reference standard ^{9}Be carrier solution (1000 ml/l) was added to all samples and to the process blank. ^{10}Be/^{9}Be ratios were measured at the Tandem Laboratory at Uppsala University. The CRONUS-Earth exposure age calculator, version 2.2, was used to calculate model ages (Balco et al. 2008; http://hess.ess.washington.edu/math/). This version of the calculator uses the revised ^{10}Be decay constant of $5.10 \pm 0.26 \times 10^{-7}$ yr^{-1} (Nishiizumi et al. 2007). Ages are presented in Table 3 and have been calculated with a regionally calibrated ^{10}Be production rate for north-eastern North America (Balco et al. 2009), which overlaps with ^{10}Be production rates reported from West Greenland (Briner et al. 2012). The scaling scheme by Lal (1991) and Stone (2000) and a constant production rate model (2σ, sea level, high latitude and standard atmosphere) have been used. Correction was made for altitude, shielding by the surrounding horizon and for sample thickness using exponential decrease in nuclide production using a density of 2.66 g cc^{-1}. All ages are calculated with zero erosion. We have chosen to do so because all collected pebbles have smooth surfaces and consist of resistant lithologies such as quartz or quartzite and postglacial erosion is considered to be minimal.

Table 1 Site information.

Site no.	Area	Site name	Latitude (°N)	Longitude (°W)	Data collection
1	Lejrelv	Lejrelv moraine	71.103	22.471	^{10}Be
2	Lejrelv	Umingmak moraine	71.081	22.455	^{10}Be
3	Lejrelv	Skansen mountain plateau	71.092	22.401	^{10}Be
4	Lejrelv	Centralbjerg mountain plateau	71.114	22.482	^{10}Be
5	Lejrelv	Lejrelv Valley delta at 295 m a.s.l.	71.176	22.764	OSL,[a] log
6	Lejrelv	Lejrelv Valley delta at 250 m a.s.l.	71.177	22.734	OSL, log
7	Lejrelv	Umingmak delta	71.151	22.777	OSL, log
8	Gåseelv	Gåseelv moraine, northern part	70.464	22.455	^{10}Be
9	Gåseelv	Gåseelv moraine, southern part	70.463	22.462	^{10}Be
10	Gåseelv	Nathorst Valley fan	70.819	22.719	OSL, log
11	Gåseelv	Nathorst Valley delta at 154 m a.s.l.	70.801	22.703	OSL, log
12	Gåseelv	Nathorst Valley delta at 120 m a.s.l.	70.786	22.694	OSL
13	Gåseelv	Gåseelv delta at marine limit	70.768	22.688	OSL, log

[a]OSL, optically stimulated luminescence.

OSL dating

Ten samples of glaciofluvial and glaciolacustrine sediments were collected in opaque plastic tubes that were hammered into dug-out sections. In addition, we have a sample of similar deposits from a nearby location in the Mestersvig delta (Fig. 1; Håkansson, unpubl. data), which serves as a control sample since we have independent age information from that site (see below). The tubes were stored in black plastic bags until opened under subdued orange light in the laboratory at the Nordic Laboratory for Luminescence Dating, Risø, Denmark. The fraction 180–250 μm was extracted and treated with 10% HCl, 10% H_2O_2 and concentrated HF according to standard procedure, to get pure quartz. Large (8 mm) and small (2 mm) aliquots were analysed using a single-aliquot regenerative-dose protocol (Table 2; see. Murray & Wintle 2000, 2003) on automated Risø TL/OSL readers (Risø, Technical University of Denmark; Bøtter-Jensen et al. 2000). Equivalent doses were calculated using the Risø software package Analyst, version 3.24; only aliquots with test dose error $<10\%$ and a recycling ratio within 10% of unity were accepted. Environmental dose rates were determined by gamma spectrometry (Murray et al. 1987), and the cosmic ray component was included according to Prescott & Hutton (1994). Water content was measured by weighing the samples with their natural water content, when saturated and when dried (Pusch 1973). A water content value halfway between the water content at the time of sampling and the saturation value was used for age calculations.

Radiocarbon dating

Four radiocarbon ages from or near our sites were retrieved from the published literature to provide independent chronological control for our ^{10}Be and OSL ages and to add to our reconstruction (Table 2). Three of these samples (Lu-647, -712 and -764) are from Kong Oscar Fjord, north of our study areas (Fig. 1). Sample Lu-764 gives the age of the local marine limit in Fleming Fjord close to the outer coast (35–60 m a.s.l., Håkansson 1974; Hjort 1979). Samples Lu-647 and Lu-712 (Håkansson 1973, 1974) were taken close to Mestersvig and provide constraints on the deglaciation of this site. Sample K-1916 (Funder 1978) provides a minimum age of the deglaciation of southernmost Klitdal and likely a close age of the marine limit in the inner Hurry Fjord, which we have sampled for OSL at site 13 (Fig. 2).

The radiocarbon ages have been calibrated by us in the OxCal 4.1 program using the IntCal09 calibration curve (Bronk Ramsey 2009; Reimer et al. 2009) after correcting the marine samples for a reservoir age of 550 years (Hjort 1973).

Landforms and sediments

Lejrelv area

On the southern side of the Umingmakelv and Draba Sibiricaelv valleys, there are discontinuous lateral meltwater channels at levels between ca. 500 and ca. 200 m a.s.l. (Figs. 2a, 3a). The channels dip 1–1.5° towards the west.

Sites 1 and 2 are on segmented ridges, ca. 20 m tall, found at ca. 300 m a.s.l. in the Umingmakelv Valley and at ca. 290 m a.s.l. in the Lejrelv Valley (Figs. 2, 3a, b). The ridges form arc-shaped features in the valleys and their surfaces are covered mainly by local sandstone cobbles, but a few crystalline and quartzite erratics <0.3 m in diameter occur. Some of the sandstone clasts are ventifacts. These ridges are interpreted as moraines, and they have subsequently been cut by the river (Figs. 2a, 3a–c). Crystalline and quartzite erratics are also scattered on the Skansen (site 3; Fig. 3d, e) and Centralbjerg mountain plateaus (site 4; Fig. 3f).

Sites 5 and 6 are river sections situated at two of several flat-topped landforms that occur in the Lejrelv Valley on levels between ca. 300 and 250 m a.s.l. along the Lejrelv River (Figs. 2a, 4a; see Lilliesköld & Salvigsen 1991). These sites are situated inboard of the moraine

Table 2 Relevant radiocarbon ages from the literature.

Site	Material	Sample no.	Age (^{14}C yr B.P.)[a]	Corrected age[b] (^{14}C yr B.P.)	Calibrated age (cal yr B.P., 2σ)[c]	Reference
I. Mestersvig: Segldal	*Hiatella arctica*	Lu-647	9610 ± 95	9060 ± 95	10 495–9912	Håkansson 1973; Hjort 1979
II. Traill Ø: Gudenelv	*Hiatella arctica*	Lu-712	9980 ± 95	9430 ± 95	11 091–10 417	Håkansson 1973; Hjort 1979
III. Fleming Fjord: Henrik Möller	*Mya truncata*, *Hiatella arctica*	Lu-764	9880 ± 95	9330 ± 95	10 779–10 246	Håkansson 1973; Hjort 1979
IV. Klitdal: Morten Sø	Organic lake sediments	K-1916	9630 ± 120		11 244–10 605	Funder 1978

[a]Radiocarbon years before the present.
[b]Reservoir correction 550 years (Hjort 1973).
[c]Calibrated by us using OxCal 4.1 and IntCal 09 (Bronk Ramsey 2009; Reimer et al. 2009). Cal yr B.P. is calibrated years before the present.

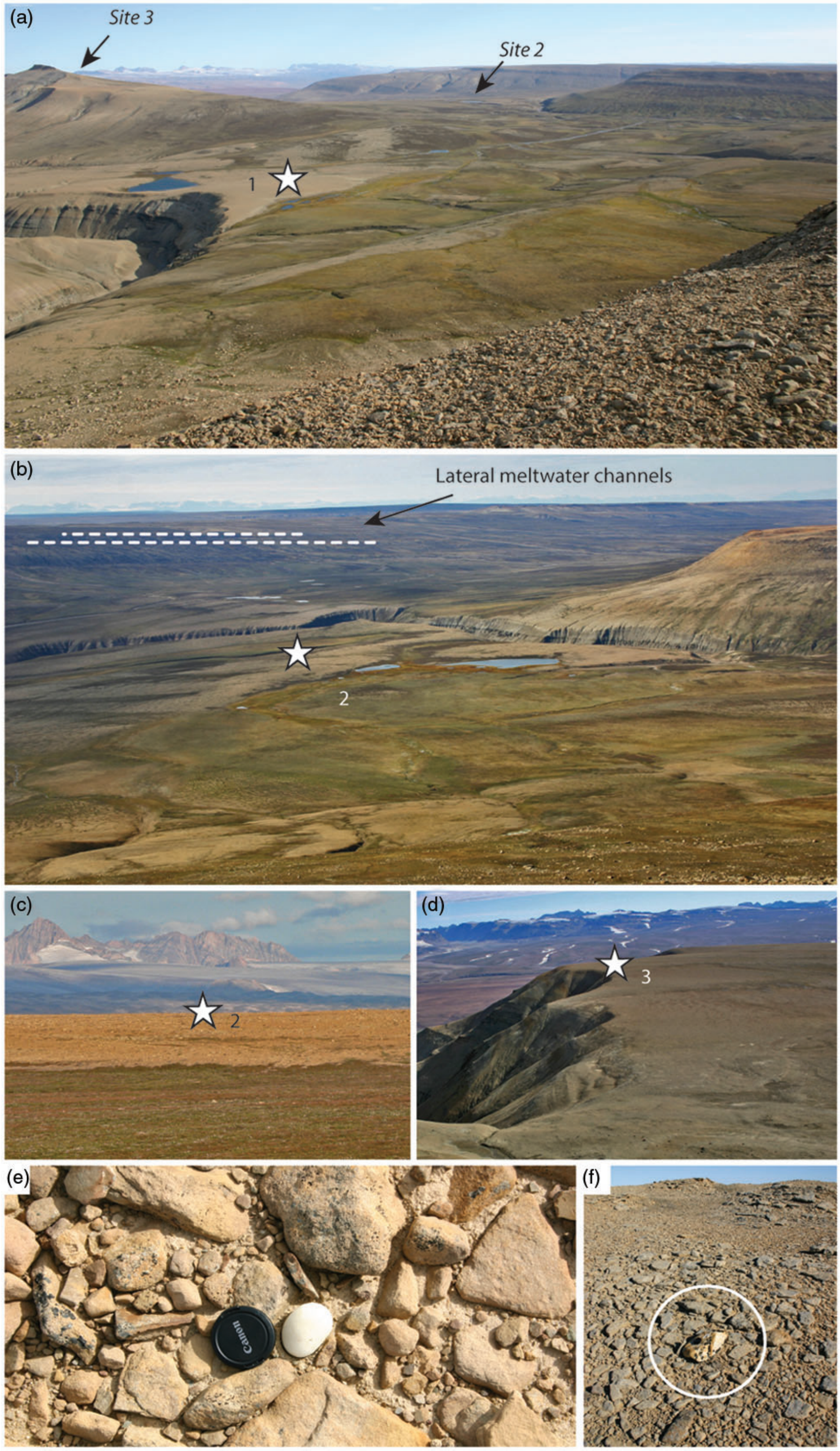

Fig. 3 (*Continued*)

Citation: *Polar Research* 2014, *33*, 20313, http://dx.doi.org/10.3402/polar.v33.20313

ridge (site 1). At site 5, the landform's top surface is at 295 m a.s.l. and sediment thickness is ca. 8 m. Sediments show a coarsening-upward succession from ripple-laminated sandy silt and sand, over planar cross-bedded sand to massive gravelly sand, finishing with a gravel lag on top (Fig. 4b). The beds dip up to ca. 15° towards the south-east, out of the valley. Site 6 at 250 m a.s.l. exhibits a sediment thickness of ca. 10 m, most of which was difficult to access due to scree cover. In the upper part of the sediment succession, the beds dip ca. 10° towards the south-east, i.e., out of the valley (Fig. 4c). They are dominated by ripple-laminated and planar parallel-laminated sand, with laminated silt at the base of the logged section.

Silty–sandy sediments are exposed in a river section between ca. 240 and 250 m a.s.l. at site 7 (Fig. 4d) in the area between the Lejrelv and Umingmak valleys and the Umingmak and Skansen mountains (Fig. 2a). This site is situated outboard of the moraine ridges at sites 1 and 2. Near the base of the sedimentary section, clayey and silty massive beds alternate with ripple-laminated sand. Upwards the succession is dominated by planar parallel-laminated and ripple-laminated sand, with a slight coarsening-upward trend. The beds dip ca. 10° towards the south-west, towards the south and the Umingmakelv Valley.

The finer, laminated sediments that dominate the successions at sites 5–7 are interpreted as being deposited by low-density turbidity currents along gentle delta slopes. The thin layers of clay and silt at site 7 were deposited during periods of breaks in sediment input from the delta slopes, likely in a deeper part of a lake. The massive gravelly sand at the top of sites 6 and 7 is interpreted as a supra-aquatic deposit, likely formed through alluvial processes, and which has later been affected by deflation to form a lag on the present surface.

Based on the geomorphology and the sediments, the landforms at sites 5–7 are interpreted as glaciolacustrine deltas. The sediment successions represent infilling of glacial lake basins in the Lejrelv Valley and, on the other side of a bedrock threshold, in the intervalley area (Fig. 2a). For lakes to form in these areas, glaciers from Liverpool Land must have dammed the present day mouths of the Umingmak and Lejrelv valleys. However, as shown by the palaeocurrent measurements, the main sediment input was not from these glaciers but from the head area of the river Lejrelv.

Gåseelv and Nathorst valleys

Sites 8 and 9 are situated on a prominent wide flat-crested ridge (ca. 130 m a.s.l.) that stretches across the Gåseelv Valley (Figs. 2b, 5). Its surface is covered mostly by local sandstone but crystalline pebbles and cobbles are common, and a few small crystalline and basalt boulders are scattered on the surface. The ridge is interpreted as a moraine. Funder (1990) mapped another moraine at ca. 400 m a.s.l. on the southern valley side, but in this study we note that this ridge is a bedrock structure.

Site 10 in the innermost Nathorst Valley is a sediment accumulation with a slightly elongated shape and its highest point at ca. 180 m a.s.l. The landform has an uneven top surface, which is gently sloping downvalley (Fig. 6a–c). The surface is covered with a lag that contains particles up to 40 cm in size, but most are 2–5 cm in diameter. A sediment section in the lower, southern part of the landform is dominated by sub-horizontal planar parallel-laminated sand. Ripple-laminated sand becomes increasingly common upwards in the sequence. Palaeocurrent directions are variable, but are mainly from the surrounding mountain slopes. The sediments below the logged section, which are largely covered by scree, appear to be gravelly. The logged sediments are interpreted as deposited by running water, likely in rather shallow channels on a glaciofluvial fan. This interpretation is supported by the palaeocurrent directions from the surrounding mountain slopes and by the gently sloping top surface of the landform. The landform may be related to a similar feature on the western side of the valley (Fig. 6a).

Downvalley of site 10, there is a flight of flat-topped landforms at levels from ca.160 to 110 m a.s.l. (Figs. 2b, 6a, d–f; see Lilliesköld & Salvigsen 1991). The sediments in these landforms are represented by a short section in one of the middle-level deltas, site 11, at 154 m a.s.l. (Fig. 6d–e). The beds, which are mainly of planar parallel-laminated medium and coarse sand, dip ca.15° towards the south, out of the valley. A few beds with ripple-laminated fine–medium sand and massive silt also occur.

Fig. 3 The Lejrelv area. White stars mark the sites from which ^{10}Be samples have been collected, numbers refer to site numbers (Table 1). (a) The Lejrelv moraine (site 1). The photograph also shows the location of the Umingmak moraine (site 2) and the Skansen mountain plateau (site 3). (b) A view into the Umingmakelv Valley from the Skansen mountain. The white star shows the location of site 2, where pebble sample CF-9 was collected. The lateral meltwater channels are located on the farther valley side, part of them marked with hatched lines. (c) The moraine in the Umingmakelv Valley (site 2). The glaciers of Liverpool Land are seen in the background. (d) The Skansen mountain (site 3). (e) Erratic pebbles and cobbles are scattered on the summit plateau of the Skansen mountain which is made up by weathered sandstone. The photograph shows the position of one of the pebbles in sample CF-4. (f) Weathered sandstone on the Centralbjerget mountain plateau (site 4). Sandstone tors are seen at the horizon. The quartzite boulder within the white circle (sample CF-7) has a long axis of ca. 0.3 m.

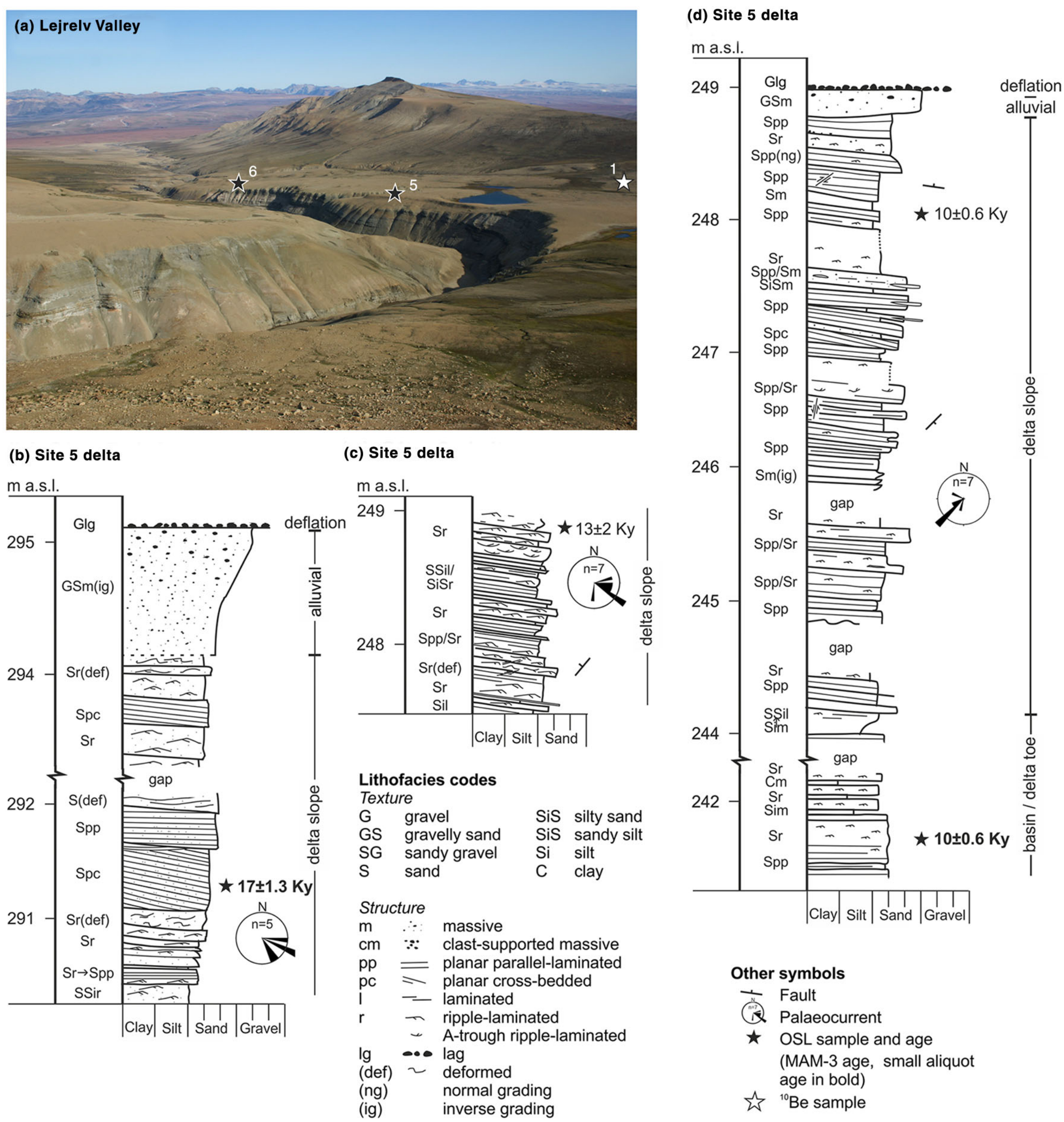

Fig. 4 Lejrelv Valley. (a) View out of the valley, towards the east, with Klitdal and Liverpool Land in the background. Stars and numbers mark site locations (see Table 1). (b). Sediment section from site 5, one of the deltas in the Lejrelv Valley, with a top surface at 295 m a.s.l. (c) Sediment section from site 6, a delta with a top surface at 250 m a.s.l. (d) Sediment section from site 7 between the Lejrelv and Umingmakelv valleys (see Fig. 2a for location). Minimum age model is abbreviated to MAM-3.

Below the logged section, there was coarse sand which appeared to be cross-bedded. A fossil ice wedge was found in finer sediments close to the top. Similar sediments were observed at the mouth of the valley at site 12, 110 m a.s.l. (Fig. 6f). The sediments are interpreted to have been formed mainly by high- and low-density turbidites flowing along a subaqueous slope. The flat-topped landforms in the Nathorst Valley are interpreted as glaciolacustrine deltas in lakes dammed by a Liverpool Land glacier. The highest delta was deposited as the glacier front was at or close to the Gåseelv moraine. The successively lower delta levels between sites 11 and 12 represent a lowering of the water level in the ice-dammed lake as the glacier retreated from the moraine.

The lowermost landform described is site 13, located at the mouth of the Gåseelv Valley at 33 m a.s.l. (Figs. 2b, 7a). The sediments show a coarsening-upward trend from massive silt and sand over planar parallel-laminated sand to clast-supported massive gravel (Fig. 7b). The sandy beds dip ca.12° towards the east and the Hurry Fjord.

Citation: *Polar Research* 2014, *33*, 20313, http://dx.doi.org/10.3402/polar.v33.20313

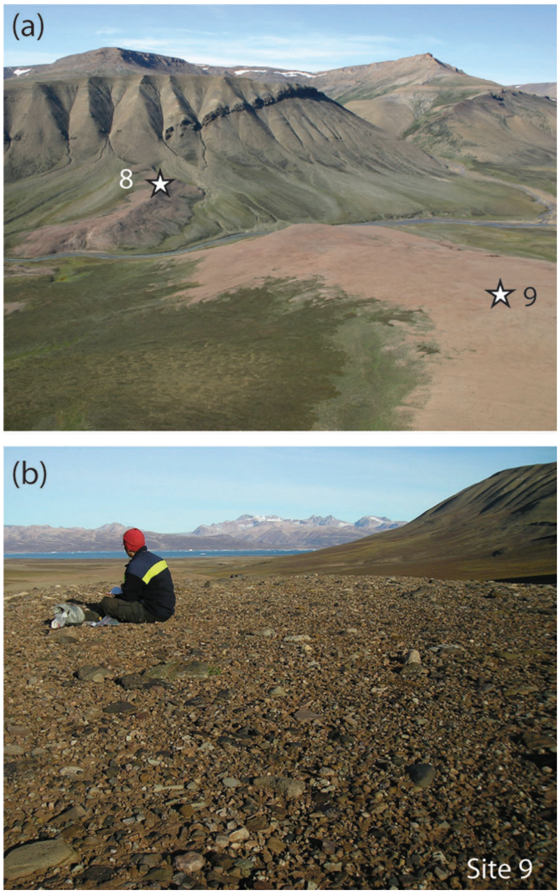

Fig. 5 Gåseelv. (a) The moraine in the Gåseelv Valley looking towards the north. Site 8 is situated at the northern and site 9 at the southern segment of the moraine. The valley in the upper right corner is the Nathorst Valley. (b) Site 9, the surface where sample GE-1 was collected. The view is towards the east with the Hurry Fjord and Liverpool Land in the background.

The sediment succession is interpreted as representing a transition from turbidites and gravity flows on a delta slope to a glaciofluvial delta top. The gravel lag at the top is caused by deflation, and soil processes have altered the uppermost decimetres below the ground surface. We suggest that this delta at 33 m a.s.l. represents the marine limit in the inner Hurry Fjord.

Chronology

Cosmogenic exposure dating

A total of eight samples were collected from mountain plateaus and from the crests of moraine ridges in east-facing valleys on eastern Jameson Land and analysed for cosmogenic ^{10}Be (Table 3).

In the Lejrelv area (Fig. 2a), a quartzite boulder perched at ca. 600 m a.s.l. on weathered sandstone bedrock on the Centralbjerg mountain plateau gives an age of 111.1 ± 7.1 Ky. Two pebble samples from the southern plateau edge of the Skansen mountain at ca. 500 m a.s.l. give ages of 13.3 ± 2.0 and 11.2 ± 2.4 Ky (site 3; Fig. 3d–e; Table 3). Pebble samples from the segmented Lejrelv- and Umingmakelv moraines at ca. 300 m a.s.l. are 6.0 ± 0.5 and 9.5 ± 1.1 Ky, respectively (site 1–2; Table 3).

In the Gåseelv area (Fig. 2b), one single cobble and two pebble samples were collected from the surface of the prominent Gåseelv moraine at ca. 130 m a.s.l. The single cobble gives an age of 4.3 ± 0.5 Ky and ^{10}Be ages from pebble samples are 8.5 ± 1.2 and 12.1 ± 3.3 Ky (sites 7–8; Table 3).

OSL dating results

The quartz has a clear fast signal component but is not very bright; the natural signals integrated over the first 0.8 s average ca. 4500 counts for small aliquots and about 30 000 counts for large aliquots (40–1000 counts/Gy). Tests with known laboratory doses show that the selected protocols are able to recover given doses within 10% (dose recovery ratio 0.91 ± 0.01, $n = 45$). Most results show significantly skewed dose distributions (Fig. 8a) and following the decision protocol of Bailey & Arnold (2006), we use the minimum age model (MAM) with three parameters (Galbraith et al. 1999; Excel macro from Sebastien Huot) to calculate the final dose for these samples. The mean ages range from ca. 10 to 50 Ky (doses 20–90 Gy) and for single samples small and large aliquot ages agree within 2σ (Table 4). The MAM-3 ages have a tighter age span (10–35 Ky), but the agreement between small and large aliquot ages is not as good (Table 4). It should be noted that the proportion of aliquots used for the MAM-3 age calculation is low for some of the small-aliquot samples (p-values in Table 4), which indicates an increased uncertainty of the accuracy.

Relative depositional history

Lejrelv area

The position of the quartzite boulder at ca. 600 m a.s.l. on the Centralbjerg plateau (site 4) and the crystalline erratics at ca. 500 m a.s.l. on the Skansen plateau (site 3) indicate minimum thickness of ice when this material was deposited. The lateral meltwater channels, at levels between ca. 500 and ca. 200 m a.s.l., reflect a successive lowering of an ice surface and an eastward retreat of the ice margin, towards Liverpool Land.

The moraines in the Umingmakelv and Lejrelv Valleys (sites 1–2) mark a younger ice-marginal position, situated east of the water divide at ca. 300 m a.s.l. This ice

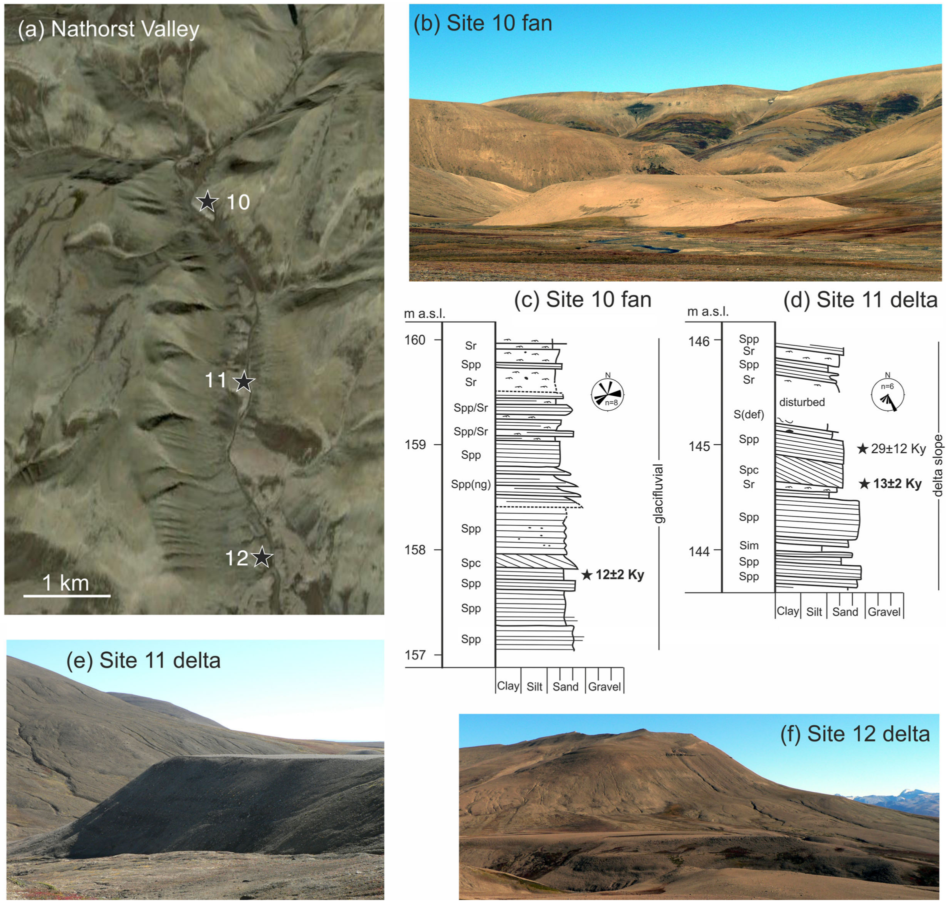

Fig. 6 Nathorst Valley. (a). Overview of the Nathorst Valley (image from Google Earth). Between sites 11 and 12 there are a series of deltas at successively lower levels. (b) A northward view of erosional remnants of a fan in the innermost part of the valley (site 10). (c) Sediment section from site 10, in the southern part of the fan shown in (b). (d) Sediment section at site 11. This delta was deposited as the Liverpool Land-based glacier's front was at or close to the Gåseelv moraine, so the optically stimulated luminescence (OSL) age is a close estimate of the formation of the moraine. (e) A south-facing photograph of one of the deltas in the middle part of the valley, this one with a top surface at 154 m a.s.l. (site 11). (f) An eastward view of the site 12 delta at 110 m a.s.l. at the mouth of the valley (site 12). See Fig. 4 for lithofacies codes.

configuration led to a lake being dammed between the Umingmakbjerg, Centralbjerg and Skansen mountains (Fig. 2). As the ice margin retreated further towards the east, ice-dammed lakes formed in the major valleys at successively lower levels (300–250 m a.s.l.). Deltas (sites 5–7) were deposited in these lakes and palaeocurrent directions show that the material in the deltas did not come from the ice in the east, but was transported from surrounding areas (Figs. 2a, 4).

Gåseelv

When the ice stood at the moraine in the Gåseelv Valley (130 m a.s.l.), a lake was probably dammed between the ice margin and the water divide 13 km to the west. Glaciolacustrine sediments mapped on the valley floor by Lilliesköld & Salvigsen (1991) support this interpretation (Fig. 2b). A lake was also dammed in the tributary Nathorst Valley to a level at least corresponding to the level of the site 11 delta (ca. 154 m a.s.l.). As the ice margin retreated towards the east, the lake was successively lowered; the lowest delta in the Nathorst Valley is at ca. 110 m a.s.l. When the valley was entirely deglaciated and open towards Hurry Fjord, a delta (site 13) was formed at the marine limit (ca. 33 m a.s.l.).

Absolute chronology: a discussion

Cosmogenic exposure dating

In the studied valleys and on the adjacent mountain plateaus, only few stable-looking boulders were observed and we have therefore chosen to collect pebble samples each of which is made up of 20 clasts. In a study in

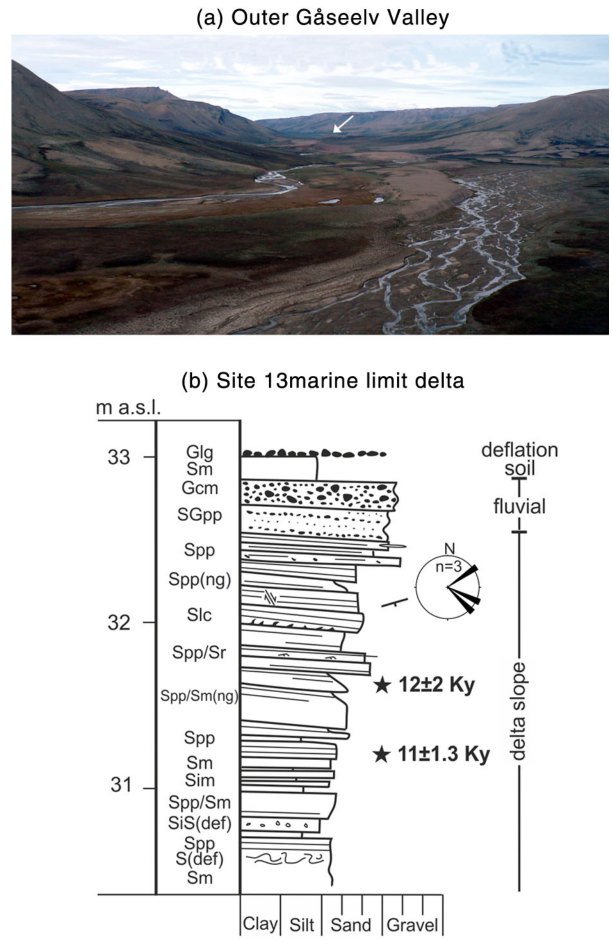

Fig. 7 The mouth of the Gåseelv Valley. (a). Erosion remnants of the marine limit delta (site 13). The cross-valley moraine (sites 8–9) is visible in the back, as indicated by the arrow. (b) Sediment section from Site 13, the marine limit delta. See Fig. 4 for lithofacies codes.

Colorado, Briner (2009) compared boulder and pebble ^{10}Be ages from the same moraines. It was shown that on Colorado moraines the two sample types produce indistinguishable exposure ages and consequently it was suggested that pebble collection on moraine crests can serve as a suitable sample type in some settings.

It has been suggested that the oldest exposure ages from moraines should be regarded as minimum constraining ages of moraine ridge formation, because degradation of landforms leads to exhumation of boulders and clasts at the surface (Putkonen & Swanson 2003; Heyman et al. 2011). Our data set is scattered and exhibits a large range of exposure ages from the moraine ridges on eastern Jameson Land (4.3–12.1 Ky, Table 3). This scatter is most probably due to incomplete exposure of pebbles caused by exhumation of clasts from the moraine and we therefore regard 12.1 ± 3.3 and 9.5 ± 1.1 Ky, the oldest ages, as minimum constraining ages of the Gåseelv moraine (sites 8–9) and the Lejrelv–Umingmakelv moraines (sites 1–2), respectively.

It should also be noted that crystalline and quartzite erratics on Jameson Land can originate either from sources west of Scoresby Sund or from Liverpool Land (Fig. 1). Those of our sampled erratics that are from moraines can by geomorphology be inferred to derive from Liverpool Land (see Fig. 2), but the sampled erratics on the mountains in the Lejrelv area are not related to any landforms indicating from which direction they were deposited. However, previous studies suggest that the last time the Greenland Ice Sheet deposited material on central and eastern Jameson Land was during the penultimate glacial cycle, about 160 Kya (Möller et al. 1994; Håkansson et al. 2009). In contrast, during the last glacial cycle Liverpool Land-based glaciers advanced onto eastern Jameson Land (Adrielsson & Alexanderson 2005) and local ice caps with limited erosion potential covered and shielded central Jameson Land for substantial periods (Håkansson et al. 2009; Håkansson et al. 2011). Due to shielding by non-erosive ice, erratics deposited ca. 160 Kya on Jameson Land will be expected to have exposure ages younger than the initial deglaciation age.

OSL dating

In glacial settings like our study area, incomplete bleaching of sediments can be a problem for OSL dating (e.g., Fuchs & Owen 2008). Based on comparisons between quartz and feldspar luminescence ages and radiocarbon ages, Hansen et al. (1999) showed that incomplete bleaching may be of the order of a few thousand years for Holocene deltaic sediments in this area. In comparison, modern fluvial sediments on Jameson Land seem better bleached with only a ca. 500-year age overestimate (Alexanderson 2007). Although the sediments we sampled in the deltas did not come directly from beneath the glaciers, but rather were transported towards them from the surroundings, the risk of incomplete bleaching should not be overlooked. Typical results of incompletely bleached deposits are skewed dose distributions, age overestimation and stratigraphically scattered ages, all of which can be checked for.

In this study, studies of dose distributions and comparisons with independent age control showed that our samples do suffer from incomplete bleaching. Dose distributions from large aliquots are not very useful for this purpose, since too much averaging occurs between the many grains in large aliquots to reliably recognize different dose populations of grains (Duller 2008), but the data from our small-aliquot measurements show that dose distributions are significantly skewed (Fig. 8).

Table 3 Sample details and ^{10}Be ages.

Sample	Latitude (°N)	Longitude (°W)	Elevation (m a.s.l.)	Site[a] no.	Sample type	Lithology	Carrier weight[b] (mg)	Quartz weight (g)	Sample thickness (cm)	Shielding correction	^{10}Be/^{9}Be not blank corrected (10^{-13}) ±error (2σ)	^{10}Be/^{9}Be[c] blank (10^{-14}) ±error (2σ)	^{10}Be[d] (10^{4} atoms s g^{-1}) ±error (2σ)	^{10}Be age[e,f] (Ky) ±error (2σ)
10-CF-2	71.0918	22.4016	497	3	20 pebbles	Quartzite	353.1	40.08	7	0.994	1.93±0.32	3.00±0.82	9.60±1.37	13.3±2.0
10-CF-4	71.0917	22.4001	505	3	20 pebbles	Quartzite	356.9	34.58	7	0.99	1.48±0.32	3.00±0.82	8.15±1.67	11.2±2.4
13-CF-5	71.1026	22.4707	301	1	20 pebbles	Gneiss	350.0	40.31	8	0.996	0.94±0.14	3.18±0.10	3.60±0.21	6.0±0.5
10-CF-7	71.1144	22.4823	595	4	Boulder	Quartzite	357.3	40.14	3	1	15.40±0.67	3.00±0.82	89.86±3.50	111.1±7.1
10-CF-9	71.0808	22.4552	286	2	20 pebbles	Gneiss	355.5	40.72	3	1	1.30±0.19	3.00±0.82	5.83±0.64	9.5±1.1
13-GE-1	70.4625	22.4616	124	9	20 pebbles	Gneiss	327.2	40.09	3	1	1.47±0.41	3.18±0.10	6.28±1.67	12.1±3.3
13-GE-3	70.4641	22.4552	127	8	Single cobble	Quartz	350.6	40.14	7	1	0.68±0.15	3.18±0.10	2.19±0.25	4.3±0.5
13-GE-5	70.4641	22.4552	127	8	20 pebbles	Gneiss	357.2	40.11	3	1	1.07±0.20	3.18±0.10	4.46±0.60	8.5±1.2

[a]Location of sites are shown in Fig. 2.
[b]Weight of SPEX CertiPrep reference standard ^{9}Be carrier solution (^{9}Be concentration: 1000 ml/l).
[c]Samples are dissolved in different batches and have thus been corrected for the specific blank of each batch.
[d]Isotopic concentrations are not corrected for elevation, latitude and shielding.
[e]Model ages are calculated with no erosion and standard pressure.
[f]Reference ^{10}Be production rate due to spallation 3.93±0.19 atoms g^{-1} yr^{-1}, based on the north-eastern North American calibration data set (Balco et al. 2009) and the standard scaling scheme of Lal (1991) and Stone (2000).

The mean dose therefore does not give a representative value of the true equivalent dose, and thus the age, but rather overestimates it. Our mean OSL ages, both for large and small aliquots, must therefore be regarded as maximum ages of the time of deposition.

To get a more representative estimate of the true dose (age) from skewed distributions, some statistical treatment, such as the MAM (Galbraith et al. 1999), is required. The good correspondence between MAM-3 ages and independent age control shows that the MAM-3 provides reliable ages, at least for small aliquots, despite the uncertainty due to low p-values (Table 4). The OSL ages of the deltas at Mestersvig (11 ± 1.4 Ky) and in Gåseelv (11 ± 1.3, 12 ± 2 Ky; Table 4) agree well with the radiocarbon ages that provide close ages for their formation (11.1–10.2 and 11.2–10.6 calibrated thousand years [cal Ky] B.P., respectively; Table 2). The MAM-3 ages from large aliquots do not show such good correspondence, which is expected due to averaging between grains (see above), and because the number of aliquots per sample is not enough for statistic certainty.

The implication is that mean ages from large aliquots of samples like these may overestimate the true age by up to ca. 20 Ky, although commonly less (average 7 Ky for our 10 samples; Table 4). Mean ages from small aliquots may also overestimate the true age (see Fig. 8a), but statistical methods such as the MAM-3 can be successfully applied to yield good results. Of our OSL ages (Table 4), we therefore find the small-aliquot MAM-3 ages most reliable.

Implications for glacial history

Our results show that outlet glaciers from the coastal Liverpool Land ice cap advanced westward and reached ice-marginal positions marked by moraines in valleys on eastern Jameson Land sometime during the late glacial–early Holocene time (ca. 13–11 Kya). This confirms our hypothesis that the east Jameson Land moraines correlate with the Milne Land Stade described elsewhere in the Scoresby Sund region (Funder 1970, 1978, 1990; Denton et al. 2005; Kelly et al. 2008). Our possibility to distinguish between an "outer" and "inner" Milne Land Stade is limited by the uncertainties and scatter of the ages (Tables 3, 4). However, in combination with the geomorphological evidence, we can discuss possible scenarios for the glacial history in the Lejrelv and Gåseelv areas.

In the Lejrelv area, we can distinguish between three glacial events: (1) an older event when ice covered the Centralbjerget plateau at 600 m a.s.l.; (2) a younger event when ice reached at least 500 m a.s.l. and deposited erratics on the Skansen plateau; and (3) the youngest

Citation: *Polar Research* 2014, *33*, 20313, http://dx.doi.org/10.3402/polar.v33.20313

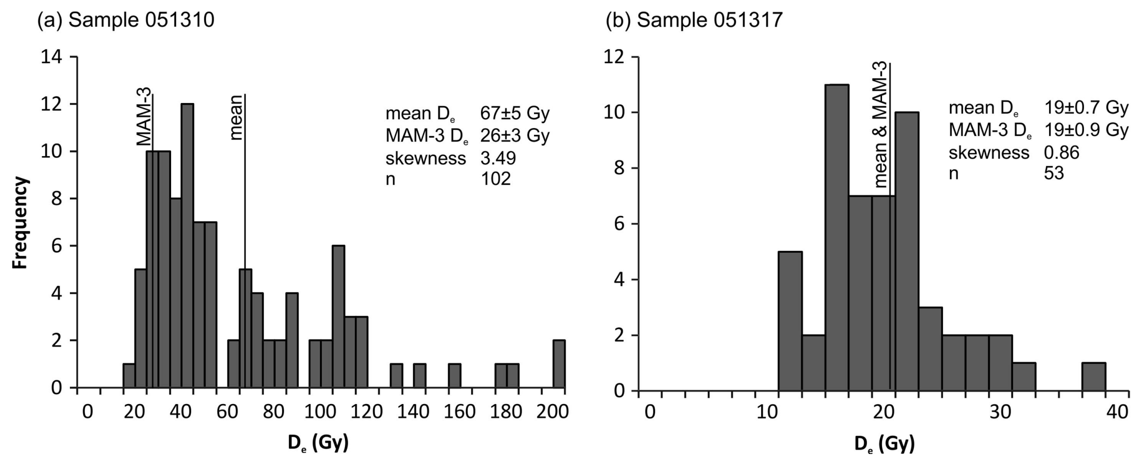

Fig. 8 Example of small-aliquot dose distributions with lines indicating the mean and minimum age model (MAM-3) doses. (a) Sample 051310. The distribution is clearly skewed with a high-dose tail and the mean value therefore does not provide a good estimate of the true equivalent dose. The MAM-3 dose, on the other hand, matches the dose expected from back-calculating from independent age control (ca. 26 Gy). (b) Sample 051317 is less skewed and the mean and MAM-3 doses fall within error of each other.

glacial event when the margin of Liverpool Land-based glaciers stood at the Umingmakelv/Lejrelv moraines (Fig. 9). The lateral meltwater channels likely represent the retreat between the two latter ice-marginal positions.

The oldest event (Fig. 9, event 1) is dated by the boulder on the Centralbjerg plateau, which gives a ^{10}Be exposure age of 111.1 ± 7.1 Ky. This age can be explained in at least two ways: either it was deposited by the Greenland Ice Sheet during MIS 6 (ca. 160 Kya) and was subsequently shielded by non-erosive ice for a total of ca. 50 Ky or it was deposited by glaciers from Liverpool Land advancing onto Jameson Land early in the last glacial cycle (Adrielsson & Alexanderson 2005).

^{10}Be exposure ages of the Skansen erratics indicate that the Skansen mountain plateau was deglaciated between 13.3 ± 2.0 and 11.2 ± 2.4 Kya (Fig. 9, event 2). A Liverpool Land-based ice reaching at least 500 m above the present sea level at Skansen must have reached far into the valleys and crossed the water divide. This implies that the meltwater at that time drained towards the west coast of Jameson Land, through the Draba Sibiricaelv and Depotelv valleys (Figs. 1, 2a, 9). This glacial event is further constrained by radiocarbon ages on raised deltas (mean age 11.8 ± 0.5 cal Ky B.P.) along the west coast of Jameson Land at the mouths of Draba Sibiricaelv, Lollandselv and Falsterselv rivers (Fig. 1; Hansen et al. 1999; Hansen 2001). The deltas were built up of material from the interior of Jameson Land, and to get sufficient amounts of water and sediment from that direction, the presence of glaciers providing meltwater to the west of the Jameson Land water divide is required. Previous studies indicate that Jameson Land-based ice was gone by this time (Adrielsson & Alexanderson 2005; Håkansson et al. 2009, 2011) and therefore the most likely source is Liverpool Land-based glaciers advancing onto Jameson Land.

The extent of Liverpool Land-based glaciers during the youngest event in the Lejrelv area is marked by the Lejrelv and Umingmak moraines. It is constrained in time between the oldest of the ^{10}Be ages (from the moraines), which are considered minimum ages, and the youngest of the OSL ages (from glacial lake sediments), which are considered maximum ages. This gives event 3 a minimum age of 9.5 ± 1.1 Ky (site 2, ^{10}Be; Table 3) and a maximum age of 10 ± 0.6 Ky (site 7, OSL; Table 4). However, based on our data we cannot tell whether the dated moraines were formed during stillstand following event 2 or by a separate advance of Liverpool Land-based glaciers.

In the Gåseelv area, the low level of the moraine and its position further east of the water divide led to the formation of ice-dammed lakes in the Gåseelv and Nathorst valleys. This event is dated to 12–13 ± 2 Kya (sites 10–11, OSL; Table 4), which corresponds to the minimum age of ca. 12 ± 3 Ky, concluded from both the ^{10}Be age of the Gåseelv moraine (sites 8–9, discussed above Table 3), and by the OSL ages of the Gåseelv marine limit delta (12–11 Ky, site 13; Table 4).

In both of our study areas, we therefore have evidence of advances of Liverpool Land-based glaciers around ca. 12 Kya (Fig. 9, event 2). In the northern area (Lejrelv), a younger event also occurred (Fig. 9, event 3) but no traces of such an event are found in the southern area (Gåseelv). This may be due to a combination of ice dynamics and topography, which is different between the areas. Once the ice margin had retreated from the

Table 4 Optically stimulated luminescence data.

Sample no.	Site no. and name	Deposit	Depth (m)	MAM-3 dose[a]	Mean dose (Gy)	*n*	Dose rate (Gy/Ky)	w.c. (%)	Protocol[b]	Mean age (Ky)	MAM-3 age[a] (Ky)	*p*[a]
					Large aliquots (8 mm)							
043042	Mestersvig	Delta at marine limit	2.0	32.6 ± 1.1	33.9 ± 1.2	29 (30)	2.49 ± 0.10	19	A	14 ± 0.8	13 ± 0.7	0.9
051307	5 Lejelv 295 m	Glaciolacustrine delta	7.3	39.9 ± 7.9	86.8 ± 13.2	13 (21)	2.06 ± 0.08	24	A	42 ± 7	19 ± 4	0.2
051315	6 Lejrelv 250 m	Glaciolacustrine delta	1.0	34.8 ± 6.1	52 ± 5.6	16 (28)	2.59 ± 0.10	15	C	20 ± 2	13 ± 2	0.1
051308	7 Umingmak	Glaciolacustrine delta	1.0	24.0 ± 1.1	25.6 ± 0.8	19 (23)	2.38 ± 0.09	18	A	11 ± 0.6	10 ± 0.6	0.4
051317	7 Umingmak	Glaciolacustrine delta	9.0	20.9 ± 0.9	22.1 ± 1	18 (21)	1.94 ± 0.08	21	A	11 ± 0.7	11 ± 0.7	0.9
051309	10 Nathorst 180 m	Glaciolacustrine delta	2.5	36.5 ± 1.1	42.3 ± 2.3	24 (24)	1.83 ± 0.07	20	B	23 ± 1.6	20 ± 1.1	0.8
051319	11 Nathorst 154 m	Glaciolacustrine delta	2.8	52.7 ± 21.4	68.2 ± 9.5	15 (18)	1.82 ± 0.07	25	A	38 ± 6	29 ± 12	0.7
051310	11 Nathorst 154 m	Glaciolacustrine delta	10.0	43.0 ± 6.9	65.5 ± 6.3	17 (21)	1.94 ± 0.08	25	A	34 ± 4	22 ± 4	0.1
051323	12 Nathorst 110 m	Glaciolacustrine delta	14.0	67.9 ± 11.6	96.8 ± 10.8	9 (12)	2.12 ± 0.09	25	A	46 ± 6	32 ± 6	0.2
051314	13 Gåseelv	Delta at marine limit	1.5	46.4 ± 2.0	51.6 ± 3.3	20 (24)	2.29 ± 0.09	21	B	22 ± 1.8	20 ± 1.3	0.8
051322	13 Gåseelv	Delta at marine limit	2.0	38.8 ± 6.0	38.6 ± 2.3	8 (9)	2.55 ± 0.09	26	B	15 ± 1.1	15 ± 2	0.5
					Small aliquots (2 mm)							
043042	Mestersvig	Delta at marine limit	2.0	28.2 ± 3.1	33.1 ± 0.8	94 (132)	2.49 ± 0.10	19	A	13 ± 0.7	11 ± 1.4	0.02
051307	5 Lejrelv 295 m	Glaciolacustrine delta	7.3	34.9 ± 2.3	95.1 ± 4.7	152 (168)	2.06 ± 0.08	24	A	46 ± 3	17 ± 1.3	0.03
051317	7 Umingmak	Glaciolacustrine delta	9.0	18.8 ± 0.9	19 ± 0.7	53 (96)	1.94 ± 0.08	21	A	10 ± 0.6	10 ± 0.6	1.00
051309	10 Nathorst 180 m	Glaciolacustrine delta	2.5	21.3 ± 2.7	46.2 ± 4.7	51 (90)	1.83 ± 0.07	20	B	25 ± 3	12 ± 2	0.02
051310	11 Nathorst 154 m	Glaciolacustrine delta	10.0	25.9 ± 3.0	66.8 ± 5.1	102 (177)	1.94 ± 0.08	25	A	34 ± 3	13 ± 2	0.02
051314	13 Gåseelv	Delta at marine limit	1.5	28.1 ± 4.6	51.9 ± 5.6	37 (84)	2.29 ± 0.09	21	B	23 ± 3	12 ± 2	0.17
051322	13 Gåseelv	Delta at marine limit	2.0	27.9 ± 3.0	49.8 ± 3.3	44 (99)	2.55 ± 0.09	26	B	20 ± 1.5	11 ± 1.3	0.03

[a] Calculated with the minimum age model (MAM-3) with three parameters (Galbraith et al. 1999; Excel macro from Sebastian Huot); *P* is the proportion of aliquots that is meaningful according to the model. If *P* is close to zero, the MAM-3 age may not be meaningful.

[b] Single-aliquot regeneration protocols (Murray & Wintle 2000, 2003). A: blue stimulation (470 ± 20 nm) at 125°C, detection in 290–370 nm (Hoya U340), preheat 220°, cut heat 200°; B: post-infrared (IR) blue stimulation (ca. 880 nm and 470 ± 20 nm) at 125°C, detection in 290–370 nm (Hoya U340), preheat 220°, cut heat 200°; C: Pulsed post-IR blue stimulation (ca. 880 nm and 470 ± 20 nm) at 125°C, detection in 290–370 nm (Hoya U340), preheat 220°, cut heat 200°.

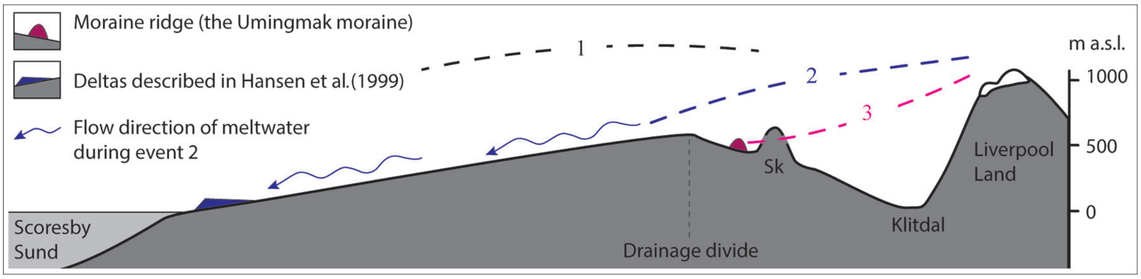

Fig. 9 Schematic cross-profile of Jameson Land illustrating the relative extent of the three glacial events described in this study: events 1, 2 and 3. Skansen mountain is abbreviated to Sk.

Gåseelv Valley, it would change into a marine calving ice margin in Hurry Fjord which, due to rapid break-up, may have prevented a re-advance. In contrast, in the north, the glacier from Liverpool Land would have been land-based in the Klitdal Valley during its retreat from the Lejrelv and Umingmakelv valleys, which could have made it easier to re-advance. Further, Lowell et al. (2013) present ^{10}Be ages from sites to the east of the Gåseelv area suggesting that Liverpool Land-based glaciers had retreated to close to close to the maximum Holocene position by 11.7 Kya.

As mentioned above, we know from other areas that the Milne Land Stade had two phases: an early (outer) and a later (inner) stage (Funder 1978; Kelly et al. 2008). Considering the time window for the presence of glaciers on eastern Jameson Land given by our ^{10}Be and OSL ages, it seems reasonable to assume that the two events we have recognized correspond to the two stages of the Milne Land Stade. Our ages of the two stages, ca. 13–11 Ky (Gåseelv area) and ca. 12–9.5 Ky (Lejrelv area), match the ages determined for the outer and inner Milne Land Stade moraines by Kelly et al. (2008) in the inner Scoresby Sund fjord: 13.0–11.6 and 11.7–10.6 Ky, respectively. We suggest that the Gåseelv moraine and the deltas in the Nathorst Valley correspond to the outer Milne Land Stade, whereas moraines and ice-dammed lakes in the Lejrelv area record the younger, slightly less extensive inner Milne Land Stade. The scatter of the presented dataset complicates the differentiation between the outer and inner Milne Land Stade. However, our results confirm the correlation of these moraines with the Milne Land Stade moraines described elsewhere in the Scoresby Sund region.

Conclusions

We have investigated and dated sediments and landforms on eastern Jameson Land related to the youngest Liverpool Land-based glacial advance. Our OSL and ^{10}Be ages indicate one older and one younger event roughly constrained to 13–11 and 12–9.5 Kya, respectively, which matches previously determined ages for the outer and inner Milne Land Stade moraines in the Scoresby Sund area. We acknowledge that our data set is small; however, combined with chronological and geomorphological information it allows us to confirm the correlation of the eastern Jameson Land moraines with the Milne Land moraine belt.

Acknowledgements

Fieldwork on Jameson Land was made possible through grants from the Swedish Society for Anthropology and Geography, the Helge Ax:son Johnson Foundation, the Royal Physiographic Society in Lund, Japetus Stenstrup's Foundation and the Swedish Royal Academy of Sciences. NordForsk financed HA's stay at the Nordic Laboratory for Luminescence Dating. Our sincere thanks go to all colleagues who have contributed to this study with discussions and technical help. We especially thank Lena Adrielsson, Christian Hjort, Sebastien Huot, Andrew S. Murray and Kristina J. Thomsen.

References

Adrielsson L. & Alexanderson H. 2005. Interactions between the Greenland Ice Sheet and the Liverpool Land coastal ice cap during the last two glaciation cycles. *Journal of Quaternary Science 20*, 269–283.

Alexanderson H. 2007. Residual OSL signals from modern Greenlandic river sediments. *Geochronometria 26*, 1–9.

Bailey R.M. & Arnold L.J. 2006. Statistical modelling of single grain quartz De distributions and an assessment of procedures for estimating burial dose. *Quaternary Science Reviews 25*, 2475–2502.

Balco G., Briner J., Finkel R.C., Rayburn J.A., Ridge J.C. & Schaefer J.M. 2009. Regional beryllium-10 production rate calibration for late-glacial northeastern North America. *Quaternary Geochronology 4*, 93–107.

Balco G., Stone J.O., Lifton N.A. & Dunai T.J. 2008. A complete and easily accessible means of calculating surface exposure ages or erosion rates from ^{10}Be and ^{26}Al measurements. *Quaternary Geochronology 3*, 174–195.

Björck S., Rundgren M., Ingólfsson Ó. & Funder S. 1997. The Preboreal oscillation around the Nordic seas: terrestrial and lacustrine responses. *Journal of Quaternary Science 12*, 455–465.

Bøtter-Jensen L., Bulur E., Duller G.A.T. & Murray A.S. 2000. Advances in luminescence instrument systems. *Radiation Measurements 32*, 523–528.

Briner J.P. 2003. *The last glaciation of the Clyde Region, northeastern Baffin Island, Arctic Canada: cosmogenic isotopes constraints on Laurentide Ice Sheet dynamics and chronology*. PhD thesis, University of Colorado.

Briner J.P. 2009. Moraine pebbles and boulders yield indistinguishable ^{10}Be ages: a case study from Colorado, USA. *Quaternary Geochronology 4*, 299–305.

Briner J.P., Young N.E., Goehring B.M. & Schaefer J.M. 2012. Constraining Holocene ^{10}Be production rates in Greenland. *Journal of Quaternary Science 27*, 2–6.

Bronk Ramsey C. 2009. Bayesian analysis of radiocarbon dates. *Radiocarbon 51*, 337–360.

Carr S.J., Lukas S. & Mills S.C. 2010. Glacier reconstruction and mass-balance modelling as a geomorphic and palaeoclimatic tool. *Earth Surface Processes and Landforms 35*, 1103–1115.

Denton G., Alley R., Comer G. & Broecker W. 2005. The role of seasonality in abrupt climate change. *Quaternary Science Reviews 24*, 1159–1182.

Duller G.A.T. 2008. Single-grain optical dating of Quaternary sediments: why aliquot size matters in luminescence dating. *Boreas 37*, 589–612.

Fuchs M. & Owen L.A. 2008. Luminescence dating of glacial and associated sediments: review, recommendations and future directions. *Boreas 37*, 636–659.

Funder S. 1970. Notes on the glacial geology of eastern Milne Land. *Rapport Grønlands Geologiske Undersøgelse 30*, 37–42.

Funder S. 1972. Remarks on the Quaternary geology of Jameson Land and adjacent areas, Scoresby Sund, East Greenland. *Rapport Grønlands Geologiske Undersøgelse 48*, 93–98.

Funder S. 1978. *Holocene stratigraphy and vegetation history in the Scoresby Sund area, East Greenland. Grønlands Geologiske Undersøgelse Bulletin 129*. Copenhagen: Geological Survey of Denmark and Greenland.

Funder S. 1990. *Descriptive text to Quaternary map of Greenland 1:500,000, Scoresby Sund, sheet 12*. Copenhagen: Geological Survey of Denmark and Greenland.

Funder S. & Hansen L. 1996. The Greenland ice sheet—a model for its culmination and decay during and after the last glacial maximum. *Bulletin of the Geological Society of Denmark 42*, 137–152.

Funder S., Hjort C. & Landvik J.Y. 1994. The last glacial cycles in East Greenland, an overview. *Boreas 23*, 283–293.

Funder S., Hjort C., Landvik J.Y., Nam S.I., Reeh N. & Stein R. 1998. History of a stable ice margin East Greenland during the middle and upper Pleistocene. *Quaternary Science Reviews 17*, 77–123.

Galbraith R.F., Roberts R.G., Laslett G.M., Yoshida H. & Olley J.M. 1999. Optical dating of single and multiple grains of quartz from Jinmium rock shelter, northern Australia. Part I: experimental design and statistical models. *Archaeometry 41*, 339–364.

Håkansson S. 1973. University of Lund radiocarbon dates VI. *Radiocarbon 15*, 493–513.

Håkansson S. 1974. University of Lund radiocarbon dates VII. *Radiocarbon 16*, 307–320.

Håkansson L., Alexanderson H., Hjort C., Möller P., Briner J.P., Aldahan A. & Possnert G. 2009. Late Pleistocene glacial history of Jameson Land, central East Greenland, derived from cosmogenic ^{10}Be and ^{26}Al exposure dating. *Boreas 38*, 244–260.

Håkansson L., Briner J.P., Aldahan A. & Possnert G. 2011. ^{10}Be data from meltwater channels suggest that Jameson Land, East Greenland, was ice-covered during the last glacial maximum. *Quaternary Research 76*, 452–459.

Håkansson L., Briner J., Alexanderson H., Aldahan A. & Possnert G. 2007. ^{10}Be ages from coastal northeast Greenland constrain the extent of the Greenland Ice Sheet during the last glacial maximum. *Quaternary Science Reviews 26*, 2316–2321.

Hall B., Baroni C., Denton G., Kelly M.A. & Lowell T. 2008. Relative sea-level change, Kjove Land, Scoresby Sund, East Greenland: implications for seasonality in Younger Dryas time. *Quaternary Science Reviews 27*, 2283–2291.

Hansen L. 2001. Landscape and coast development of a lowland fjord margin following deglaciation, East Greenland. *Geografiska Annaler 83A*, 131–144.

Hansen L., Funder S., Murray A.S. & Mejdahl V. 1999. Luminescence dating of the last Weichselian glacier advance in East Greenland. *Quaternary Geochronology 18*, 179–190.

Heyman J., Stroeven A.P., Harbor J.M. & Caffee M.W. 2011. Too young or too old: evaluating cosmogenic exposure dating based on an analysis of compiled boulder exposure ages. *Earth and Planetary Science Letters 302*, 71–80.

Hjort C. 1973. A sea correction for East Greenland. *Geologiska Föreningen i Stockholms Förhandlingar 95*, 132–134.

Hjort C. 1979. Glaciation in northern East Greenland during the Late Weichselian and Early Flandrian. *Boreas 8*, 281–296.

Kelly M.A. & Lowell T.V. 2009. Fluctuations of local glaciers in Greenland during latest Pleistocene and Holocene time. *Quaternary Science Reviews 28*, 2088–2106.

Kelly M.A., Lowell T.V., Hall B.L., Schaefer J.M., Finkel R.C., Goehring B.M., Alley R.B. & Denton G.H. 2008. A ^{10}Be chronology of lateglacial and Holocene mountain glaciation in the Scoresby Sund region, East Greenland: implications for seasonality during lateglacial time. *Quaternary Science Reviews 27*, 2273–2282.

Kohl C.P. & Nishiizumi K. 1992. Chemical isolation of quartz for measurement of in-situ-produced cosmogenic nuclides. *Geochimica et Cosmochimica Acta 56*, 3583–3587.

Lal D. 1991. Cosmic ray labeling of erosion surfaces: in situ nuclide production rates and erosion models. *Earth and Planetary Science Letters 104*, 424–439.

Citation: *Polar Research* 2014, *33*, 20313, http://dx.doi.org/10.3402/polar.v33.20313

Leclercq P. & Oerlemans J. 2012. Global and hemispheric temperature reconstruction from glacier length fluctuations. *Climate Dynamics 36*, 1065–1079.

Lilliesköld M. & Salvigsen O. 1991. Glacial features and stratigraphy on eastern Jameson Land. *LUNDQUA Report 33*, 111–116.

Lowell T.V., Hall B.L., Kelly M.A., Bennike O., Lusas A.R., Honsaker W., Smith C.A., Levy L.B., Travis S. & Denton G.H. 2013. Late Holocene expansion of Istorvet ice cap, Liverpool Land, East Greenland. *Quaternary Science Reviews 63*, 128–140.

Möller P., Hjort C., Adrielsson L. & Salvigsen O. 1994. Glacial history of interior Jameson Land, East Greenland. *Boreas 23*, 320–348.

Murray A.S., Marten R., Johnson A. & Martin P. 1987. Analysis for naturally occurring radionuclides at environmental concentrations by gamma spectrometry. *Journal of Radioanalytical and Nuclear Chemistry Articles 115*, 263–288.

Murray A.S. & Wintle A.G. 2000. Luminescence dating of quartz using an improved single-aliquot regenerative-dose protocol. *Radiation Measurements 32*, 57–73.

Murray A.S. & Wintle A.G. 2003. The single aliquot regenerative dose protocol: potential for improvements in reliability. *Radiation Measurements 37*, 377–381.

Nesje A., Bakke J., Dahl S.O., Lie Ø. & Matthews J.A. 2008. Norwegian mountain glaciers in the past, present and future. *Global and Planetary Change 60*, 10–27.

Nishiizumi K., Imamura M., Caffee M.W., Southon J.R., Finkel R.C. & McAninch J. 2007. Absolute calibration of ^{10}Be AMS standards. *Nuclear Instruments and Methods in Physics Research Section B: Beam Interactions with Materials and Atoms 258*, 403–413.

Prescott J.R. & Hutton J.T. 1994. Cosmic ray contributions to dose rates for luminescence and ESR dating: large depths and long-term time variations. *Radiation Measurements 23*, 497–500.

Pusch R. 1973. Densitet, vattenhalt och portal. (Density, water content and void ratio.) *Byggforskningens Informationsblad 5*, 27.

Putkonen J. & Swanson T. 2003. Accuracy of cosmogenic ages for moraines. *Quaternary Research 59*, 255–261.

Reimer P.J., Baillie M.G.L., Bard E., Bayliss A., Beck J.W., Blackwell P.G., Bronk Ramsey C., Buck C.E., Burr G.S., Edwards R.L., Friedrich M., Grootes P.M., Guilderson T.P., Hajdas I., Heaton T.J., Hogg A.G., Hughen K.A., Kaiser K.F., Kromer B., McCormac F.G., Manning S.W., Reimer R.W., Richards D.A., Southon J.R., Talamo S., Turney C.S.M., van der Plicht J. & Weyhenmeyer C.E. 2009. IntCal09 and Marine09 radiocarbon age calibration curves, 0–50,000 years cal BP. *Radiocarbon 51*, 1111–1150.

Stone J.O. 2000. Air pressure and cosmogenic isotope production. *Journal of Geophysical Research—Solid Earth 105*, 23753–23759.